Journal for ImmunoTherapy of Cancer

# Selection of therapeutically effective T-cell receptors from the diverse tumor-bearing repertoire

Leonie Rosenberger,[1] Leo Hansmann,[2,3] Vasiliki Anastasopoulou,[1,3] Steven P Wolf ,[4,5] Kimberley Drousch,[1] Christina Moewes,[1] Xinyi Feng,[6] Guoshuai Cao,[6] Jun Huang ,[6] Poh Yin Yew,[7] Erlend Strønen ,[8] Taigo Kato,[9] Naresha Saligrama,[10,11] Johanna Olweus,[8,12] Yusuke Nakamura,[13] Gerald Willimsky ,[1,3] Thomas Blankenstein,[14] Hans Schreiber,[4,5,15] Matthias Leisegang [1,3,5]

**To cite:** Rosenberger L, Hansmann L, Anastasopoulou V, *et al*. Selection of therapeutically effective T-cell receptors from the diverse tumor-bearing repertoire. *Journal for ImmunoTherapy of Cancer* 2025;**13**:e011351. doi:10.1136/jitc-2024-011351

► Additional supplemental material is published online only. To view, please visit the journal online (https://doi.org/10.1136/jitc-2024-011351).

Accepted 03 April 2025



For numbered affiliations see end of article.

**Correspondence to**
Matthias Leisegang;
matthias.leisegang@uchicago.edu

## ABSTRACT

**Background** The development of T-cell receptor (TCR)-based T-cell therapies is hampered by the difficulties in identifying therapeutically effective tumor-specific TCRs from the natural repertoire of a patient's cancer-specific T cells.

**Methods** Here, we mimic experimentally near-patient conditions to analyze the T-cell repertoire in euthymic tumor-bearing mice responding to the H-2K$^{b}$-presented neoantigen p68$^{S551F}$ (mp68). We temporarily separated the time point of mp68 expression from that of cancer cell transplantation to exclude the influence of injection-induced inflammation on T-cell priming. Thus, the mp68-specific T-cell response could only develop after the acute inflammatory phase had subsided.

**Results** We found that mp68-specific TCRs isolated from either tumor-infiltrating T cells or spleens of mice immunized with mp68-expressing cancer cells are diverse and not inherently therapeutic when introduced into peripheral T cells and used for adoptive therapy of established tumors. While measuring short-term T-cell responses in vitro was unreliable for some TCRs in predicting their therapeutic failure, assessing the persistence of cancer cell destruction by TCR-modified T cells in long-term cultures accurately predicted therapeutic outcomes. A tumor-derived TCR with optimal function was also correctly identified with this approach when analyzing human TCRs that recognize the HLA-A2-presented neoantigen CDK4$^{R24L}$.

**Conclusions** We show that a neoantigen-directed T-cell response in tumor-bearing hosts comprises a diverse repertoire. Infiltration and expansion of certain T-cell clonotypes in the tumor do not necessarily correlate with therapeutic efficacy of their TCRs in adoptive therapy. We propose that analysis of persistent rather than immediate responses of TCR-modified T cells in vitro serves as a reliable parameter to identify TCRs that are therapeutically effective in vivo.

### WHAT IS ALREADY KNOWN ON THIS TOPIC

⇒ Predicting the therapeutic efficacy of cancer-specific T-cell receptors (TCRs) for adoptive T-cell therapy is essential but has proven challenging due to the difficulty of extrapolating in vitro parameters.

### WHAT THIS STUDY ADDS

⇒ Here, we determined the therapeutic efficacy of TCRs in a near-clinical setting of stringent T-cell therapy to study the predictive power of preclinical analyses.

⇒ We evaluated neoantigen-specific TCRs from tumor-bearing hosts and found that TCRs from expanded T-cell clones were not all therapeutically effective.

⇒ Distinguishing failing from effective TCRs was successful by assessing the long-term persistence of T-cell products in vitro.

### HOW THIS STUDY MIGHT AFFECT RESEARCH, PRACTICE OR POLICY

⇒ The results of this study provide guidance on how to select effective immune receptors for adoptive T-cell therapy and open new research into why some TCRs of expanded tumor-specific T-cell clonotypes from patients are effective in destroying tumors while others fail.

## BACKGROUND

The T-cell receptor (TCR) that is used to engineer T cells for adoptive therapy (TCR-therapy) largely determines treatment responses, as the TCR defines the therapeutic target as well as the function of TCR-modified T cells (TCR-Ts). This also applies to TCRs recognizing antigens resulting from somatic mutations in tumor DNA that are presented by major histocompatibility complex (MHC) molecules on the cell surface.[1] These mutations are mostly caused by cancer-specific non-synonymous single nucleotide variations that result in single amino acid substitutions, also known as point mutations.[2 3] Because these aberrant proteins are not expressed during T-cell development in the thymus, they are recognized by the adult immune

system as new antigens and are therefore often referred to as neoantigens (NeoAg). Importantly, most NeoAgs are specific for the individual murine or human cancer in which they are found. Extensive studies in human cancers have shown that about 99% of these neoantigenic determinants are not shared between patients and are therefore appropriately referred to as "unique".[4]

Provided that NeoAgs are highly and homogeneously expressed in the tumor, a TCR derived from NeoAg-specific CD8 T cells seems to be sufficient to eliminate even large and established solid tumors when used for TCR therapy.[5 6] However, unmanipulated tumors often show lower NeoAg expression and are mostly characterized by heterogeneity, since they diversify genetically early in their evolution.[5 7] We have shown that targeting multiple NeoAgs with TCR-Ts can reduce the risk of therapy-induced tumor escape.[8] However, even TCR therapy using three NeoAg-specific TCRs derived from CD8 T cells was rarely effective when targeting autochthonous NeoAgs because the enormous heterogeneity of established tumors allowed antigen-negative cancer cells to escape.[8] In contrast, we further showed that two TCRs, one isolated from CD4 T cells (reactive against a cancer-derived NeoAg presented on stromal cells) and one from CD8 T cells (targeting a NeoAg on cancer cells), are essential and sufficient to eliminate large heterogeneous cancers in mice.[8]

For targeting recurrent NeoAgs, the same TCRs could be used to treat specific patient subgroups.[9] These off-the-shelf TCRs would be readily available; but, because they were not selected in the autologous host, they may carry the risk of unintended reactivity. Furthermore, the unique nature of most cancer mutations would require even more individualized treatment strategies. An approach in which autologous NeoAg-specific TCRs are isolated from the cancer patient's repertoire and used therapeutically would result in a truly personalized TCR therapy. First clinical results showed no objective or only transient therapeutic effects,[10 11] which may be attributed to omitting therapeutically effective CD4 T cells. The importance of the latter for tumor destruction has become more evident in preclinical studies.[8 12 13] In addition, predicting which patient-derived TCRs will show therapeutic efficacy prior to clinical application remains difficult. We previously showed that convergent TCR recombination can be used as an indicator for the therapeutic efficacy of tumor-derived TCRs isolated from CD4 T cells.[13]

In the current study, we pursued a functional approach to predict the therapeutic efficacy of tumor-derived TCRs experimentally. We developed a model system with inducible expression of the H-2K$^{b}$-presented NeoAg p68$^{S551F}$ (mp68)[3] that mimics obstacles faced by T cells in naturally growing tumors, such as suboptimal priming conditions due to lack of acute inflammation. Under those suboptimal priming conditions, antigenic tumors may grow to large sizes without inducing a tumor-destructive immune response and thus sneak through immune surveillance.[14 15] Furthermore, the resulting chronic antigen exposure may render any newly generated NeoAg-specific CD8 T-cell dysfunctional.[16] Thus, our model allowed us to delay antigen induction until the transplantation-induced inflammation had subsided. As in patients, the endogenous NeoAg-specific T-cell response was unable to prevent tumor progression. The mp68-specific tumor-infiltrating T cells comprised a diverse repertoire of TCR clonotypes and we tested whether expanded T-cell clones contain therapeutically effective TCRs. Only about one-half of the NeoAg-specific TCRs we isolated induced tumor destruction when expressed in peripheral T cells and adoptively transferred. Similar results were obtained when analyzing TCRs isolated from the spleens of mice immunized with mp68-expressing cancer cells. Predicting the therapeutic efficacy of TCRs in vivo required in vitro assays that assessed TCR-T persistence rather than immediate T-cell responses and antigen sensitivity. These results were confirmed in experiments comparing the therapeutic efficacy of human TCRs.

## MATERIALS AND METHODS

### Plasmids

Genes encoding mp68-specific TCRs (table 1) were designed as described (TCR-β-P2A-TCR-α),[5] synthesized (GeneArt, Thermo Fisher), and cloned into pMP71.[17] CDK4$^{R24L}$-specific TCRs (table 2) are described (14/35, P1, H1-1, H2-1, H2-2)[6 18] or were generated in this work (M1, see below). TCR genes comprising native leader sequences, and constant regions of mouse TCR-αβ counterparts[19] were cloned into pMP71. For studying TCR function in vivo, CDK4$^{R24L}$-specific TCRs were cloned into pMP71-IRES-GFP. For doxycycline-inducible expression, three sequences encoding for the mp68 epitope were separated by AAY, fused to Thy1.1 ((SNFVFAGI-AAY)$_3$-Thy1.1) and cloned in the vector pMOV[20] (pMOV-mp68-Thy1.1). For constitutive expression, (SNFVFAGI-AAY)$_3$-Thy1.1 was cloned into pMP71 (pMP71-mp68-Thy1.1). The transgene cassettes of both epitope-encoding fusion constructs started with a methionine to initiate transcription.

### Cells

Cells were cultured in Roswell Park Memorial Institute (RPMI) medium with 5% heat-inactivated fetal calf serum (FCS, PAN Biotech) and 100 U/mL penicillin/streptomycin (cell medium, CM). 8101 cancer cells are derived from a tumor that arose in an UV-irradiated C57BL/6 mouse[3]: 8101 (regressor phenotype, mp68$^{+}$), 8101PRO (progressor phenotype, mp68$^{-}$), and 8101–12 (clone 12, regressor phenotype, mp68$^{+}$). Presence or absence of mp68 was verified by sequencing as described.[7] Transduction of 8101PRO using MP71-mp68-Thy1.1 (8101PRO-mp68) and 8101–12 using MP71-GFP (8101–12-GFP) was done as described[6] followed by enrichment using flow cytometry. Relapse variants of 8101PRO-mp68 that

**Table 1** Sequences of TCR clonotypes expanded in mp68-tetramer-binding TILs of mice bearing 4E9$^{ON}$ tumors or in T cells of immune spleens after immunization with 4E9$^{ON}$ cancer cells

| | | TCR | | | | | | |
|---|---|---|---|---|---|---|---|---|
| **Mouse** | **Origin** | **Name** | **TRAV** | **TRAJ** | **CDR3 of TCR-α** | **TRBV** | **TRBJ** | **CDR3 of TCR-β** |
| 1D9 | Immune spleen | 1D9 | 1 | 30 | CAVRSDTNAYKVIF | 19 | 2–7 | CASSKRLSSYEQYF |
| T1 | TIL (3 weeks) | T1-1 | 1 | 30 | CAVRADTNAYKVIF | 19 | 2–7 | CASSIRQGSGEQYF |
| | | T1-2 | 12–2 | 30 | CALTSDTNAYKVIF | 15 | 1–3 | CASSRTGNTLYF |
| | | T1-3 | 19 | 40 | CAAGGFNTGNYKYVF | 19 | 2–7 | CASSIRQGSGEQYF |
| T2 | TIL (3 weeks) | T2-1 | 9–3 | 50 | CAVSIASSSFSKLVF | 16 | 2–1 | CASRTQGNYAEQFF |
| | | T2-2 | 16D | 53 | CAMRESSGGSNYKLTF | 13–3 | 2–4 | CASSHRLGQNTLYF |
| T3 | TIL (5 weeks) | T3-1 | 19 | 40 | CAAGGVNTGNYKYVF | 13–2 | 2–2 | CASGEAGGVTGQLYF |
| | | T3-2 | 9D-4 | 50 | CVLSAIASSSFSKLVF | 16 | 1–1 | CASSPQGNTEVFF |
| | | T3-3 | 13–4 | 30 | CAMEHDTNAYKVIF | 12–1 | 2–1 | CASSLRGYAEQFF |
| | | T3-3/2 | 19 | 40 | CAAGGVNTGNYKYVF | 12–1 | 2–1 | CASSLRGYAEQFF |
| T4 | TIL (14.5 weeks) | T4-1 | 16D | 37 | CAMREGLTGNTGKLIF | 16 | 2–4 | CASSLNPGLGGSQNTLYF |
| | | T4-2 | 19 | 40 | CAAGGVNTGNYKYVF | 19 | 2–2 | CASSILGGDTGQLYF |
| V1 | Immune spleen | V1-1 | 14D-1 | 57 | CAASDQGGSAKLIF | 13–2 | 2–4 | CASGDALGENTLYF |
| | | V1-2 | 8D-2 | 48 | CATSYGNEKITF | 1 | 2–3 | CTCSADAGRSAETLYF |
| | | V1-3 | 9–1 | 31 | CAVSASNNRIFF | 14 | 1–1 | CASNDRGRNTEVFF |
| V2 | Immune spleen | V2-1 | 9–1 | 49 | CAVKGYQNFYF | 1 | 2–7 | CTCSGDWGGSEQYF |
| | | V2-2 | 13D-2 | 23 | CAIEALNYNQGKLIF | 12–1 | 2–3 | CASSPRQALGAETLYF |
| | | V2-3 | 8–1 | 38 | CATEHNVGDNSKLIW | 16 | 1–6 | CASSRDRNSPLYF |

T3-3/2, TCR consisting of TCR-β and the secondary TCR-α chain of clonotype T3/3. For TIL-derived TCR clonotypes, the time that T cells could interact with mp68 in the tumor-bearing host is given in parentheses after origin. Information on TCR variable and joining regions, and CDR3s were obtained from the International ImMunoGeneTics database.[31]
CDR3, amino acid sequence of the complementary determining region 3, TRBV, TCR-β chain variable region; TCR, T-cell receptor; TIL, tumor-infiltrating lymphocytes; TRAJ, TCR-α chain joining region; TRAV, TCR-α chain variable region; TRBJ, TCR-β chain joining region.

occurred after TCR-therapy were seeded as single cell suspensions and kept in culture for at least three passages to remove stromal content. 8101PRO-4E9 cancer cells (4E9) were generated by transduction of 8101PRO using MOV-mp68-Thy1.1. 4E9 cancer cells were cultured for 48 hours in CM containing 500 ng/mL doxycycline to induce mp68 expression in vitro (4E9$^{ON}$). MC703 cancer cells[6] are derived from a methylcholanthrene-induced tumor of an HHD[21] mouse. MC703-ALD[6] is its derivative with constitutive expression of the ALD epitope. WM-902B+A2[6] are melanoma cells natively expressing CDK4$^{R24L}$ and with ectopic expression of HLA-A2 and GFP. Plat-E[22] and 293-RD114[23] packaging cells were used for generating

**Table 2** Sequences of TCRs targeting the HLA-A2-presented neoantigen CDK4$^{R24L}$

| | | | TCR | | | | | |
|---|---|---|---|---|---|---|---|---|
| **Name** | **Origin** | **Ref.** | **TRAV** | **TRAJ** | **CDR3 of TCRα** | **TRBV** | **TRBJ** | **CDR3 of TCRβ** |
| 14/35 | Patient PBMC | 6 39 | 20 | 58 | CAVQSGTSGSRLTF | 9 | 2–1 | CASSVVAGFNEQFF |
| P1 | Patient TIL (17) | 18 37 | 29 | 43 | CAAFLQSNDMRF | 27 | 2–1 | CASRASGREQFF |
| H1-1 | Donor T cells (53) | 18 | 8–2 | 34 | CVVSDLYNTDKLIF | 7–8 | 2–7 | CASSQNYEQYF |
| H2-1 | Donor T cells (55) | 18 | 14 | 37 | CAMSSLSGNTGKLIF | 6–5 | 2–7 | CASSYSWGAGYEQYF |
| H2-2 | Donor T cells (57) | 18 | 8–1 | 20 | CAVILRSNDYKLSF | 29–1 | 2–2 | CSAGTGELFF |
| M1 | Mouse: immune spleen | – | 12–2 | 26 | CAVNMPYGQNFVF | 29–1 | 2–3 | CSVGQGDTQYF |

The designation of the TCR clonotypes in the original publications is given in parentheses after origin. Information on TCR variable and joining regions, and CDR3s were obtained from provided references or the International ImMunoGeneTics database.[31]
CDR3, amino acid sequence of the complementary determining region 3, TRBV, TCR-β chain variable region; PBMC, peripheral blood mononuclear cells; Ref., references; TCR, T-cell receptor; TIL, tumor-infiltrating lymphocytes; TRAJ, TCR-α chain joining region; TRAV, TCR-α chain variable region; TRBJ, TCR-β chain joining region.

ecotropic or amphotropic virus supernatant, respectively. The murine T-cell line 58[24] lacks endogenous expression of TCR-αβ genes.

### T-cell culture and transduction

T cells were cultured in RPMI supplemented with 10% FCS, 1 mM sodium pyruvate, 100 µM non-essential amino acids and 50 µM 2-mercaptoethanol (T-cell medium, TCM). Transfection of packaging cells was performed with Lipofectamine (Thermo Fisher) and 3 µg of pMP71 plasmids as detailed above (see Plasmids). Virus supernatant harvested 48 hours later. Primary human T cells: $1.5\times10^6$ human peripheral blood mononuclear cells were isolated as described[6] seeded in TCM in 24-wells coated with anti-CD3 (OKT3, 5 µg/mL) and anti-CD28 (CD28.2, 1 µg/mL) antibodies 48 hours before transduction. Transduction was performed on two consecutive days by spinoculation for 90 min at 800 g and 32°C with 1 mL amphotropic virus. T cells were kept in the continued presence of human interleukin (IL)-2 (13 days at 400 U/mL, 2 days at 40 U/mL, Novartis) before being frozen and used for experiments. Primary mouse T cells: single cell suspensions of spleens of C57BL/6 or HHD mice were generated as described[6] and cultured at $2\times10^6$ cells/mL with anti-CD3 (clone: 145–2C11, 1 µg/mL), anti-CD28 (37.51, 0.1 µg/mL), and human IL-2 (40 U/mL) to activate T cells. Transduction was performed 24 and 48 hours later. For this, $1.5\times10^6$ cells were seeded in virus-coated[6] wells together with protamine sulfate (4 µg/mL, Sigma), $4\times10^5$ mouse T-Activator beads (Thermo Fisher), and IL-2 (40 U/mL) together with 1 mL ecotropic virus supernatant and spinoculated for 30 min at 32°C and 800 g. Fresh virus supernatant was added on the following day for a second spinoculation. T cells were further cultured in IL-15 (50 ng/mL, Miltenyi Biotec) and expanded for 9 days before being frozen and used for in vitro assays. For adoptive transfer, T cells were used 3 days after completing transduction and after removing T-Activator beads using a magnet. 58 cells: $1\times10^5$ cells were seeded in 24 wells, before adding ecotropic virus supernatant 24 hours and 48 hours later, each time followed by spinoculation (30 min, 32°C, 800 g). Cells were further expanded for functional assays.

### Animals

The ARRIVE reporting guidelines were followed to provide information on the use of laboratory animals.[25] Mice ($Rag^{-/-}$ (B6.129S7-*Rag1*$^{tm1Mom}$), TNA2 (B6.Cg-Tg(HLA-A/H2-D/B2M)1Bpe *H2-D1*$^{tm1Bpe}$ *B2m*$^{tm1Unc}$ *Rag1*$^{tm1Mom}$/Luck),[6] C57BL/6, HHD,[21] and AB*ab*-A2[26] were bred in a specific pathogen-free environment in the animal facility of the Max-Delbrück-Center for Molecular Medicine. Tumor induction: $3–5\times10^6$ 8101PRO-mp68, MC703-ALD,[6] or 4E9$^{OFF}$ cancer cells were injected in 100 µL phosphate-buffered saline (PBS) subcutaneously into the right flank of either $Rag1^{-/-}$, TNA2, or C57BL/6 mice (12–20 weeks old, female or male), respectively. Presence or absence of antigen expression was verified by flow cytometry assessing Thy1.1 or GFP expression prior to cancer cell injection. Tumor size was determined using a caliper three times per week according to $\pi/6\times$ (abc). Mice were sacrificed when either tumors reached the maximum permitted size, the maximum observation time was reached (150 days) or if due to tumor burden the overall health condition was poor. To compare TCR quality, the T-cell therapy experiments were designed with a group size sufficient to distinguish TCRs based on the extent of tumor regression. Examiners were not blinded with respect to treatment groups. Other potential confounders were not accounted for. Animals were excluded from analysis, if they died due to reasons unrelated to tumor burden. Immunization: C57BL/6 mice were inoculated with $3–5\times10^6$ lethally irradiated 4E9$^{ON}$ cancer cells (20 Gy). Antigen expression was confirmed by staining for Thy1.1 prior to irradiation. Doxycycline treatment of mice (see below) started 48 hours prior to tumor cell inoculation. Two consecutive boosts using live 4E9$^{ON}$ cancer cells were performed 6 and 10 weeks later. 10 days after the second boost, mice were sacrificed to isolate their spleen. TCR-M1 was generated by immunizing an AB*ab*-A2 mouse as described.[27] The mouse received three times 1–2 µg of plasmid encoding the CDK4$^{R24L}$ epitope ALD by gene gun and three times with peptide (100 µg) combined with Cytosine-phosphate-Guanine (CpG) oligonucleotides and incomplete Freund's adjuvant. The boosts were performed 1, 5, 7, 9 and 10 months after the initial immunization. 8 days after the last immunization, the mouse was sacrificed and splenocytes were cultured for 10 days in the presence of $1\times10^{-8}$ M ALD peptide and then sorted by flow cytometry using interferon (IFN)-γ capture assay as described. Adoptive T-cell transfer: mice received indicated TCR-Ts intravenously 2–4 weeks after tumor induction. Treatment groups were allocated with a similar average tumor size. TCR-Ts were used on day 5 of ex vivo culture (3 days after completing TCR transduction). The total number of transferred cells was adjusted according to the transduction rate to transfer $1\times10^6$ CD8$^+$ TCR-Ts per mouse. TCR-Ts were injected intravenously in 100 µL PBS. Control mice received unmodified T cells or no T cells. Doxycycline treatment: C57BL/6 mice bearing 3 weeks old 4E9$^{OFF}$ tumors or to receive 4E9$^{ON}$ cancer cells received 200 µg doxycycline per milliliter drinking water supplemented with 5% sucrose changed two times a week. 4E9$^{OFF}$ tumors were at least palpable at this point.

### TCR sequencing

Single T-cell sequencing: 4E9$^{ON}$ tumors were excised, homogenized (gentleMACS dissociator (Miltenyi Biotec)) and enzymatically digested in collagenase D (2 mg/mL, Roche), DNAse I (20 U/mL, Sigma) for 90 min, and additional 30 min in 0.025% trypsin at 37°C before analyzing single cell suspensions by flow cytometry. Single cell suspensions of immune spleens were viably frozen until used for analysis by flow cytometry. Cells were stained using H-2K$^b$:mp68 tetramers (PE, MBL, dilution: 1:200) and antibodies against CD8 (BV421, clone:

53–6.7, 1:100), CD3 (APC, 145–2C11, 1:50), and 7-AAD (BioLegend). Live, single $CD3^+CD8^+$ mp68-tetramer-binding cells were sorted (BD Aria Fusion) into 96-well PCR plates containing 12 µL of 1× One-Step RT-PCR buffer (Qiagen) and snap frozen on dry ice as described.[28] TCR sequences of single cells were determined according to previously published protocols.[28–30] Briefly, TCR-encoding messenger RNAs were reverse-transcribed and amplified in a PCR reaction using the One-Step RT-PCR kit (Qiagen) and TCR-specific primers.[30] Using nested primers,[30] a second PCR was performed and barcodes[28] were added in a third PCR reaction using HotStarTaq DNA polymerase (Qiagen). Amplified and barcoded TCR sequences were then pooled, gel-purified and sequenced using MiSeq Reagent Kit v2, 500 cycles (Illumina) and the Illumina MiSeq instrument for paired-end sequencing. The sequencing data were processed as described.[28] Bulk T-cell sequencing: the TCR repertoire of T cells sorted with mp68-tetramers from the tumor of mouse T1 was determined as described.[7] The identification of TCR genes from the AB*ab*-A2 mouse immunized against $CDK4^{R24L}$ was done as described.[27] Identity of TCR genes was determined using the International ImMunoGeneTics database.[31]

### Flow cytometry

Single cell suspensions of tumors (see above) or spleens were stained with anti-CD39 (APC, Duha59, 1:100), anti-PD-1 (BV711, 29F.1A12, 1:50), anti-CD8 (APC-Cy7, 53–6.7, 1:100), anti-CD3 (BV421, 145–2C11, 1:50) and 7-AAD. Appropriate isotype controls for anti-Programmed Death (PD)-1 and anti-CD39 were included for all samples. TCR expression in primary mouse TCR-Ts was assessed by staining with anti-CD8 (BV421, 53–6.7, 1:100) and antibodies detecting the variable regions of TCR-β: TCRvβ2 (B20.6, 1:10), 5 (MR9-4, 1:50), 6 (RR4-7, 1:50), 8.1 (MR5-2, 1:50), 11 (KT11, 1:50), 13 (MR12-4, 1:50) all in PE from BioLegend. TCR expression in TCR-Ts derived from primary human T cells was analyzed using anti-CD8 (BV421, 53–6.7, 1:100) and antibodies detecting the mouse constant region of TCR-β (APC, H57-597, 1:50) or using GFP when used as a marker for TCR expression (integrated via an IRES to the expression vector).[6] TCR expression in 58 cells was determined by detecting CD3 (APC, 145–2C11, 1:50) and intracellular/extracellular presence of mouse constant TCR-β (APC, H57-597, 1:50). Intracellular staining was performed using the Cytofix/Cytoperm Fixation/Permeabilization Kit (BD). Reisolated cancer cells of $4E9^{ON}$ and 8101PRO-mp68 tumors were stained with anti-Thy1.1 (APC, OX-7, 1:500) to confirm Thy1.1 expression. SYTOX Blue (BD) or 7-AAD was used to discriminate live and dead/apoptotic cells in each measurement. If not stated otherwise, antibodies were purchased from BioLegend.

### T-cell function

Short-term: 24 hours co-cultures of $5\times10^4$ TCR-Ts with target cells (Effector-to-Target ratio: 1:1) were performed in 96-well plates. Target cells were irradiated (63 Gy) splenocytes of C57BL/6 mice loaded with the indicated mp68 peptide (SNFVFAGI (purity: >95%, HPLC-purified), Biosyntan), 8101 and 8101PRO-mp68. Serial dilutions of the mp68 peptide were performed in the range of $1\times10^{-6}$ to $1\times10^{-12}$ M. Non-engineered T cells, and TCR-Ts cultured without target cells or with 1 µM ionomycin (Calbiochem) and 5 ng/mL phorbol-12-myristate-13-acetate (Promega) for TCR-independent cytokine release were used as controls. Supernatants of co-cultures were analyzed for IFN-γ content by ELISA (BD). Long-term: $2\times10^3$ tumor cells (WM-902B+A2 or 8101–12-GFP) were seeded in 96-well plates before adding $1\times10^4$ $CD8^+$ TCR-Ts 24 hours later. The total number of T cells per well was kept constant by adding non-engineered T cells. Mouse TCR-Ts were used without cryopreservation. Every 3 days, $2\times10^3$ fresh tumor cells were seeded into the wells (re-challenge). Co-cultures were analyzed by continued imaging (every 2 hours with a 10× objective) using an Incucyte SX5 (Sartorius). Outgrowth of GFP-expressing tumor cells was determined as the time when confluence reached 10% (8101–12-GFP) or 15% (WM-902B+A2).

### Statistics and software

Statistical calculations were performed using Prism V.9 (GraphPad). Fluorescence-Activated Cell Sorting (FACS) data was analyzed using FlowJo V.10 (FlowJo). SnapGene (GSL Biotech LLC) was used to analyze DNA sequences.

## RESULTS

### Endogenous mp68-specific CD8 T cells infiltrate tumor tissue but fail to prevent cancer progression

The 8101 cancer cells harbor the autochthonous NeoAg mp68 ($DDX5_{S551F}$) that induces a CD8 T-cell response when the cancer was used for immunization of C57BL/6 mice.[3] The mp68 peptide binds with high affinity to $H\text{-}2K^b$[32] and proved to be a rejection antigen for T-cell therapies targeting large established 8101 tumors with high and homogenous mp68 expression.[5] To mimic induction and prolonged exposure of T cells to mp68 in immunocompetent mice, we used the progressor tumor variant 8101PRO that was generated by serial transplantation of 8101 cancer cells into C57BL/6 hosts.[33] Due to in vivo selection, 8101PRO lost mp68 as verified by sequencing of genomic DNA (figure 1A). We reinstalled mp68 expression in 8101PRO under control of a doxycycline-inducible promoter[20] along with Thy1.1 as a surface marker. Transcription of mp68 in the derivative clone 8101PRO-4E9 (hereafter $4E9^{ON/OFF}$) was tightly controlled, as shown by doxycycline-dependent expression of Thy1.1 (figure 1B) and recognition of $4E9^{ON}$ but not $4E9^{OFF}$ cancer cells by mp68-specific TCR-Ts (figure 1C). The mp68-specific TCR for generating TCR-Ts was obtained by immunizing C57BL/6 mice with 8101 cancer cells (designated 1D9[5]). When $4E9^{OFF}$ cancer cells were injected into immunocompetent mice, most animals developed measurable tumors about 3 weeks later (online supplemental figure 1A,

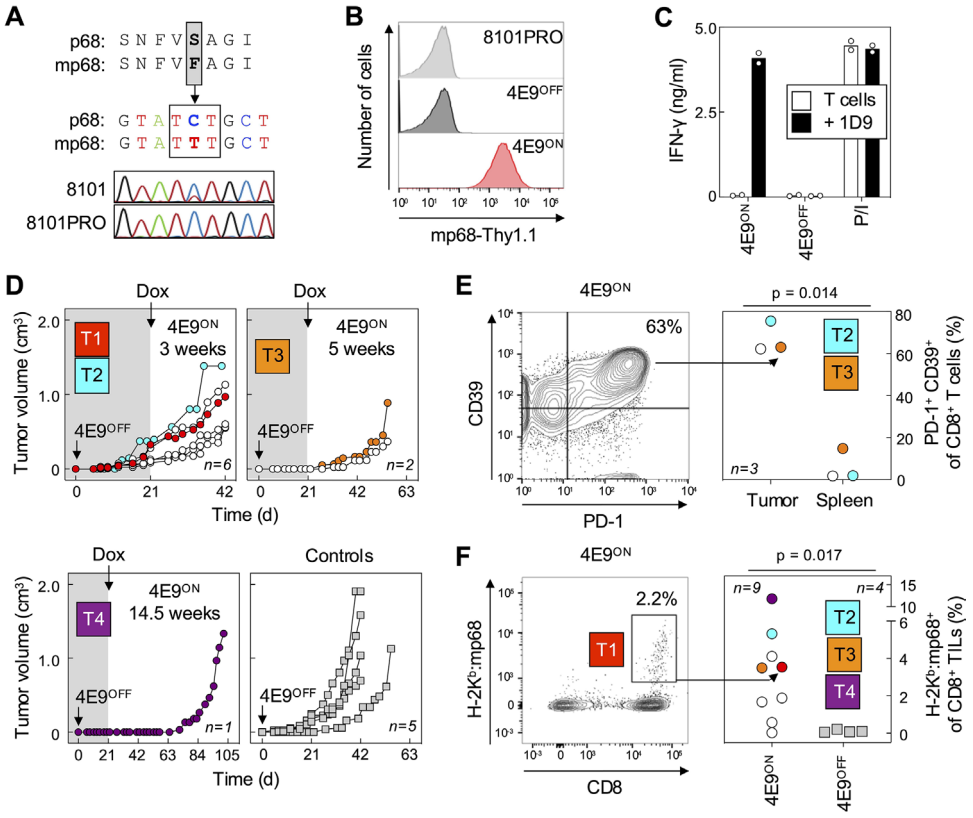


**Figure 1** Induction of mp68 neoantigen expression in a progressively growing cancer causes infiltration of mp68-specific T cells that are unable to suppress tumor growth. (A) 8101 cancer cells harbor a serine (S) to phenylalanine (F) exchange in position 551 of the p68 protein that is caused by a point mutation (cytosine to thymidine transition). Electropherograms show the presence or absence of the point mutation (red) in 8101 (mp68$^{+}$, heterozygous) and 8101PRO (mp68$^{-}$). (B) 8101PRO-derived 4E9 cancer cells are mp68$^{-}$ (4E9$^{OFF}$) and express the mp68-Thy1.1 fusion gene on incubation with doxycycline (4E9$^{ON}$). Histograms show surface expression of Thy1.1 in indicated cells as determined by flow cytometry. (C) 1D9 TCR-Ts secrete IFN-γ when incubated with 4E9$^{ON}$ but not 4E9$^{OFF}$ cancer cells. Depicted values are technical replicates of an experiment that was repeated nine times showing comparable results. P/I, phorbol-12-myristate-13-acetate/ionomycin. (D) Induction of mp68 expression cannot prevent progression of 4E9$^{ON}$ tumors in C57BL/6 mice. Data are compiled from two independent experiments and plotted on separate x-axes according to growth kinetics. Curves are shown for tumors isolated 3 weeks (upper left, mouse T1 (red) and T2 (cyan) are highlighted), 5 weeks (upper right, T3 in orange), and 14.5 weeks (lower left, T4 in purple) after inducing mp68 expression 21 days after inoculation. Other mice in the treatment group are shown as open circles. Growth of 4E9$^{OFF}$ tumors is shown as control (lower right, gray squares). (E–F) 4E9$^{ON}$-infiltrating CD8 T cells show surface markers of exhaustion (E) and contain a fraction that binds mp68-tetramers (F). CD3$^{+}$CD8$^{+}$ TILs from reisolated 4E9$^{ON}$ tumors were analyzed by flow cytometry to assess expression of CD39 and PD-1 (E) and binding of mp68-tetramers (F) using material from three to nine animals, respectively. Mice T1-T4 are color-coded. Additional mice are shown as open circles. Representative FACS plots show TILs of mouse T3 (E) and T1 (F) gated on CD3$^{+}$CD8$^{+}$ cells (left). A comparison with corresponding splenocytes (E) and TILs from 4E9$^{OFF}$ tumors (F) is shown as a scatter plot (right). The number (n) indicates the sample size for each graph. P values result from paired t-test (E) or unpaired t-test with Welch's correction (F). FACS, Fluorescence-Activated Cell Sorting; IFN, interferon; P/I, phorbol-12-myristate-13-acetate/ionomycin; PD-1, Programmed Death-1; TIL, tumor-infiltrating lymphocyte.

figure 1D). Expression of mp68 was initiated 3 weeks after transplantation, when acute inflammation at the injection site had subsided[34] and tumors were 142±132 mm$^{3}$ in size (figure 1D). However, the expression of mp68 could not prevent tumor progression, even when induced in small, only palpable 4E9 tumors (figure 1D). A comparison of 4E9$^{ON}$ and 4E9$^{OFF}$ tumors 3 weeks after induction of mp68 expression showed no significant difference in size (online supplemental figure 2). All progressing 4E9$^{ON}$ tumors were infiltrated by CD8 T cells expressing high levels of PD-1 and CD39 (figure 1E), indicating their terminally dysfunctional phenotype[35] and providing context for their failure to arrest tumor growth. A fraction of these CD8 tumor-infiltrating lymphocytes (TILs) bound a tetramer loaded with the mp68 peptide (figure 1F), thus mirroring NeoAg-specific T-cell responses observed in patients.[36] TILs isolated from progressing 4E9$^{OFF}$ tumors were unable to bind the mp68 tetramer (figure 1F).

## Endogenous mp68-specific CD8 T cells express a diverse repertoire of unique TCR clonotypes

To characterize the mp68-specific CD8 T-cell response in 4E9 tumor-bearing mice, we sorted TILs of mouse T1 (figure 1D) that bound the mp68 tetramer (figure 1F) and captured their TCR-α and TCR-β repertoire. Surprisingly, TCR loci within this T-cell population showed combinations

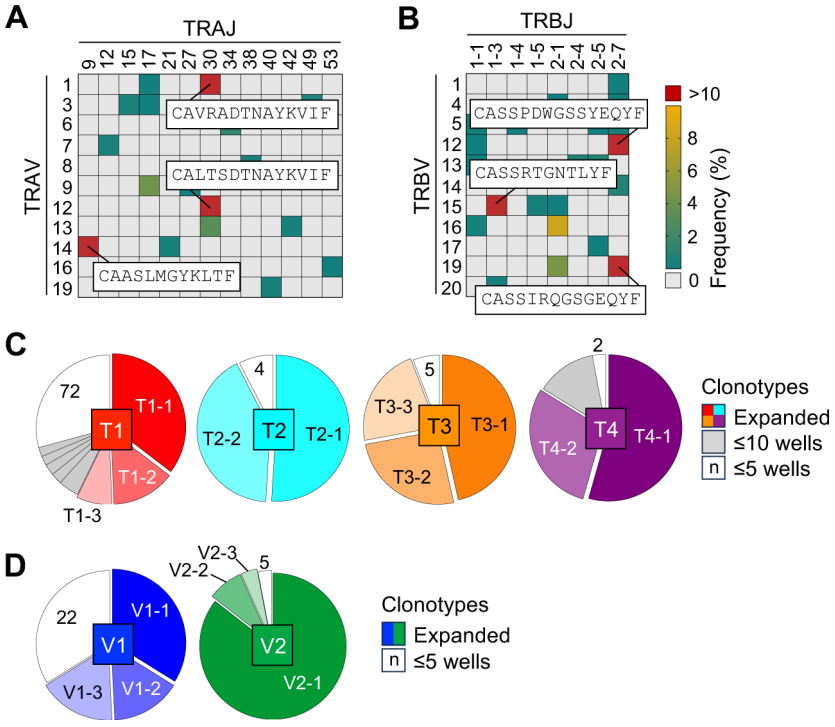


**Figure 2** T cells that bind mp68-tetramers isolated from TILs of 4E9$^{ON}$ tumors or immunized mice comprise a diverse repertoire of TCRs. (A–B) The frequency of TRAV-TRAJ (A) and TRBV-TRBJ (B) combinations found in TCR genes of TILs isolated from the 4E9$^{ON}$ tumor of mouse T1 is shown as a heat map. Combinations with a frequency above 10% in the repertoire are indicated in red and their CDR3 usage is shown. (C–D) TCR sequences of single CD8$^{+}$ T cells binding the mp68-tetramer were determined and the relative abundance of T-cell clonotypes is indicated in pie charts. T cells were isolated from 4E9$^{ON}$ tumors of mice T1 (red), T2 (cyan), T3 (orange), and T4 (purple) (C) or from spleens of 4E9$^{ON}$-immunized mice V1 (blue) and V2 (green) (D). Expanded T-cell clonotypes are color-coded and the fraction of non-expanded clonotypes, which are represented in ≤10 (C) or ≤5 wells (C-D), are indicated in gray (C) and white (C-D). The number of clonotypes contained in the non-expanded fraction is given. TCR, T-cell receptor; TIL, tumor-infiltrating lymphocyte; TRAJ, TCR-α chain joining region; TRAV, TCR-α chain variable region; TRBJ, TCR-β chain joining region; TRBV, TCR-β chain variable region.

of many different variable and joining regions (TRA: 17, TRB: 22; figure 2A,B) comprising a large number of different CDR3s (TRA: 60, TRB: 100). However, only three of the V-J combinations found in the TCR-α and TCR-β loci accounted for more than 10% of the repertoire and encoded distinct CDR3 sequences, indicating expansion of certain T-cell clonotypes (figure 2A,B). To identify the clonal ancestry of these frequent TCR genes, we sorted~180 single mp68 tetramer-binding T cells from the CD8 population of TILs and sequenced their individual TCR-αβ pairs.[29 30] As expected, the most abundant TCR-α and TCR-β genes from the repertoire analysis (figure 2A–B) were found in the majority of the single T cells (table 1), confirming the TCR identity of three expanded T-cell clonotypes (figure 2C). We continued the analysis for three additional mice by isolating single mp68-specific CD8 T cells from TILs of mouse T2 (analyzed 3 weeks after induction of mp68 expression), mouse T3 (5 weeks), and mouse T4 that was analyzed after 14.5 weeks in which T cells were exposed to mp68 in the tumor microenvironment (figure 1D, middle panels). Mouse T1, T2, T3, and T4 comprised a total of 10 expanded CD8 T-cell clonotypes, and at least two clonotypes were expanded in each mouse. The TCR sequences of the expanded T-cell clonotypes differed between and within the investigated mice, with differences characterized by usage of different variable and joining regions and largely different CDR3s (table 1). Furthermore, all non-expanded TCR clonotypes identified in the four mice (n=84) were unique and not found in TILs of another mouse. This tremendous TCR diversity was not limited to the repertoire of mp68 tetramer-binding TILs, as additional TCR clonotypes (n=33) were found in spleens of C57BL/6 mice (V1, V2) following immunization with 4E9$^{ON}$ cancer cells. The mice received lethally irradiated 4E9$^{ON}$ cancer cells and subsequently rejected live 4E9$^{ON}$ cancer cells in two consecutive boosts 6 and 10 weeks after initial immunization (online supplemental figure 1B). T cells in immune spleen cells of these mice contained three TCR clonotypes each that were expanded (figure 2D and table 1), but like all other sequences, these TCRs were again unique and not found in the other immunized mouse or in any of the mp68 tetramer-binding TILs.

### Effective and failing TCRs are found in expanded mp68-specific clonotypes of tumor-bearing or immunized mice

All TCR genes derived from CD8 T cells that expanded in response to mp68 in tumor-bearing and vaccinated mice were molecularly cloned. When introduced into TCR-negative 58 cells, all TCRs assembled with endogenous CD3 and thus supported functional TCR expression

(online supplemental figure 3A,B). TCR-Ts were similarly generated from primary T cells of C57BL/6 mice (online supplemental figure 3C). 3 of the 16 TCRs (T1-2, T1-3, and T3-3) failed to bind mp68-loaded tetramers (online supplemental figure 3C,D) and showed no reactivity when incubated with target cells loaded with mp68 peptide (online supplemental figure 3E). A second TCR-α chain found in TILs T3-3 failed to confer mp68 reactivity (TCR T3-3/2, online supplemental figure 3D,E). In TILs encoding for TCRs T1-2 and T1-3, no second subdominant TCR-α chain was found. These three non-reactive TCRs were excluded from subsequent analyses. Next, we evaluated the therapeutic efficacy of mp68-reactive TCR-Ts by treating $Rag^{-/-}$ mice that had established 8101PRO tumors that constitutively expressed a fusion gene encoding mp68 and Thy1.1, which served as a surface marker (8101PRO-mp68, online supplemental figure 1C). A small fraction of 8101PRO tumor cells (mp68-Thy1.1-negative) remained in the 8101PRO-mp68 population (online supplemental figure 4), allowing the therapeutic efficacy of the TCR-Ts to be measured by their ability to select for these cancer cell variants. Although all mp68-reactive TCRs supported antigen-specific expansion in tumor-bearing (T1, T2, T3, T4; n=7) or immunized mice (V1, V2; n=6), less than half of the analyzed TCR-Ts (n=6) were therapeutically effective

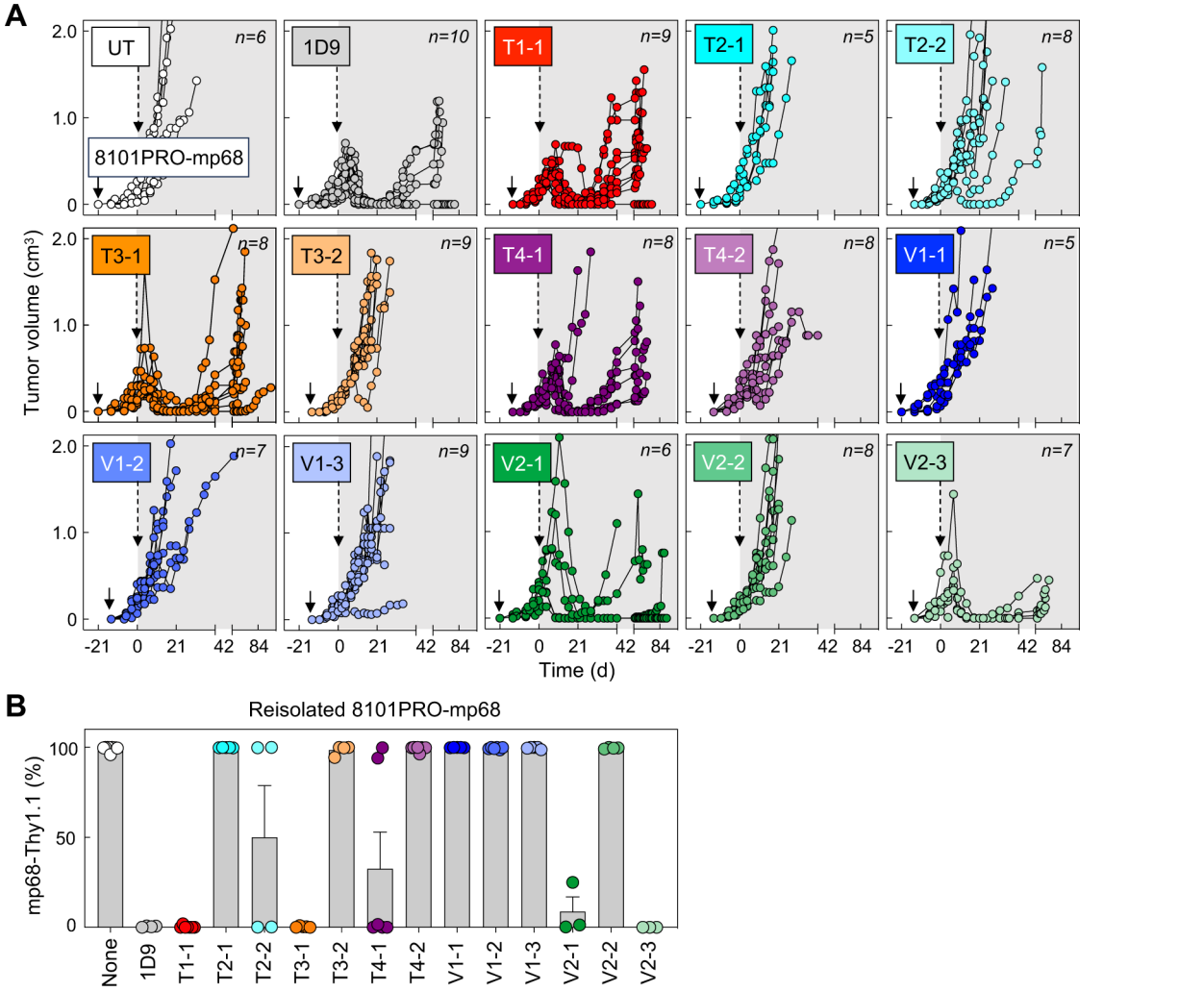


**Figure 3** Less than half of the TCRs isolated from mp68-tetramer-binding TILs or T cells of immunized mice are therapeutically effective. (A) The therapeutic quality of TCR-Ts was determined by TCR-therapy in mice bearing large established 8101PRO-mp68 tumors and is represented by their ability to destroy tumors. Shown are tumor growth curves of individual mice pooled from two to three independent experiments. The number of treated mice in each group is shown in the upper right of each graph. Injection of 8101PRO-mp68 cancer cells is indicated with an arrow. 2–3 weeks after cancer cell injection, TCR-Ts (color-coded for each originating mouse and TCR clonotype) were adoptively transferred (day 0, dashed arrows). Mice receiving unmodified T cells (UT) are shown as control. The average tumor size at treatment start was 182±103 $mm^3$. The number (n) indicates the sample size for each graph. (B) Loss of Thy1.1 expression on reisolated cancer cells of relapsing 8101PRO-mp68 tumors is indicative of treatment success. Reisolated cancer cells were adapted to culture and the percentage of $Thy1.1^+$ cells was determined by flow cytometry. Lack of $Thy1.1^+$ cells indicates the selection of $mp68^-$ escape variants by the respective TCR-Ts. Each data point represents one tumor. Mean and SEM are shown. TCR-Ts, T-cell receptor-modified T cells; TIL, tumor-infiltrating lymphocyte.

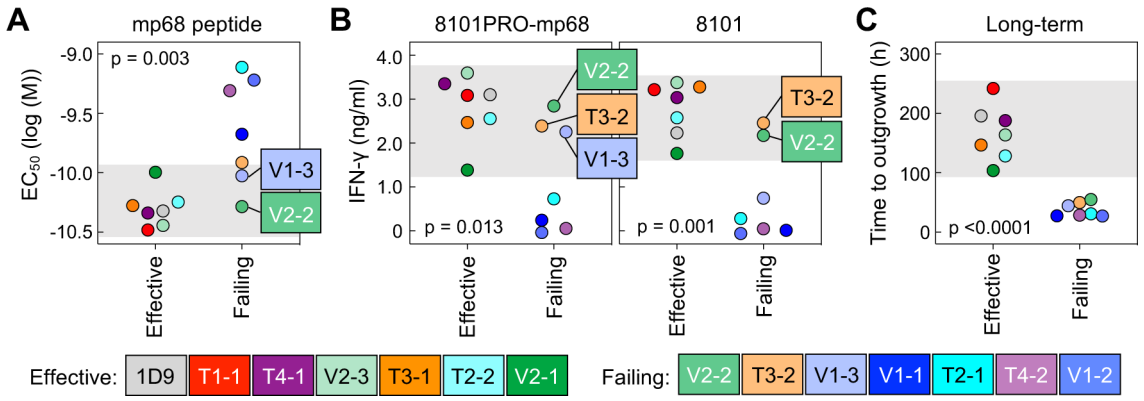


**Figure 4** Long-term, but not short-term in vitro assays are accurate predictors of in vivo efficacy of mp68-specific TCR-Ts. TCR-Ts expressing mp68-specific TCRs derived from TILs of 4E9$^{ON}$ tumors or immunized mice were incubated with splenocytes loaded with graded amounts of mp68 peptide (A), 8101 cancer cells with ectopic (B, left) or native expression of mp68 (B, right and C). TCRs were classified as effective or failing based on their in vivo efficacy (figure 3) and are represented as single dots showing an average of three to eight independent experiments (detailed in online supplemental figure 5). (A) $EC_{50}$ is the concentration of mp68 peptide required to elicit half-maximal IFN-γ release by TCR-Ts when loaded on splenocytes in 24 hours co-cultures. (B) IFN-γ release by TCR-Ts was determined after 24 hours co-culture with 8101PRO-mp68 (left) or 8101 cancer cells (right). (C) TCR-Ts were incubated with 8101–12-GFP cancer cells and time to tumor outgrowth (≥10% confluence) was assessed by monitoring co-cultures using Incucyte SX5. Additional 8101–12-GFP cancer cells were added to the culture every 3 days. The range of the data set for therapeutically effective TCRs is indicated in gray. Failing TCRs that fall within this range are indicated. P values result from unpaired t-tests. IFN, interferon; TCR-Ts, T-cell receptor-modified T cells; TIL, tumor-infiltrating lymphocyte.

(figure 3). Therapeutic efficacy was indicated by tumor regression (figure 3A) and recurrence of mp68-Thy1.1-negative cancer cell variants (figure 3B). In three treatment groups (T2-2, T4-1, V2-1), the varying percentage of mp68-Thy1.1-negative cancer cell variants in the reisolates aligned with the therapeutic outcome observed in the individual mice (figure 3A,B). The therapeutically effective cluster of TCRs included those from TILs (n=4) and immunized mice (n=2), with one TCR from each group (T1-1, V2-1) achieving tumor eradication in a fraction of treated mice, suggesting that the therapeutic quality of NeoAg-specific TCRs derived from TILs was not inferior to that of TCRs isolated from tumor-free environments. Importantly, one but not all of the isolated TCRs from each of the four tumor-bearing mice were therapeutically effective, necessitating preliminary screening to avoid treatment failure.

## Therapeutic efficacy of TCR-Ts is predicted by their persistent control of tumor growth in vitro

The activation profile of TCR-Ts after incubation with target cells either loaded with graded amounts of mp68 peptide (figure 4A) or endogenously expressing mp68 at high (8101PRO-mp68, figure 4B, left) or natural (8101, figure 4B, right) levels revealed a significant difference between the group of therapeutically effective and failing TCRs. These data were derived from four to eight individual experiments (online supplemental figure 4A–C), which demonstrated reproducibility but also inherent variations across repetitions. A cluster of three failing TCRs (V2-2, V1-3, T3-2) showed an activation profile that overlapped with the group of therapeutically effective TCRs (figure 4, online supplemental figure 5), making them difficult to discriminate. We therefore evaluated the long-term persistence of antitumor activity by repeatedly challenging TCR-Ts with tumor cells (online supplemental figure 6). Similar to the control of cancer progression in vivo, we monitored whether outgrowth of 8101 cancer cells (8101–12-GFP) could be prevented by TCR-Ts in vitro. Indeed, the time that TCR-Ts could inhibit tumor progression in cell culture was found to be an accurate predictor of therapeutic efficacy in vivo (figure 4C, online supplemental figure 5D). Importantly, the cluster of three failing TCRs that was incorrectly suggested to induce robust antitumor responses by short-term assays was also clearly identified as ineffective when TCR-T persistence was used as a parameter (figure 4C, online supplemental figure 5D).

## CDK4$^{R24L}$-specific TCRs from patients are therapeutically effective

We extended the analysis to a set of human TCRs targeting an HLA-A2-presented NeoAg derived from mutant CDK4 (CDK4$^{R24L}$, table 2). A TIL-derived CDK4$^{R24L}$-specific TCR (hereafter referred to as P1)[37] was compared with several TCRs obtained from tumor-free settings: (1) CDK4$^{R24L}$-specific TCRs were generated by in vitro stimulation of T cells of healthy donors. For this, dendritic cells of two donors (H1, H2) were loaded with CDK4$^{R24L}$-encoding RNA and used to prime and expand autologous T cells in cell culture.[38] TCRs from derivative clones of these T-cell lines (hereafter referred to as H1-1, H2-1, and H2-2) have been described.[18] (2) We further isolated a TCR

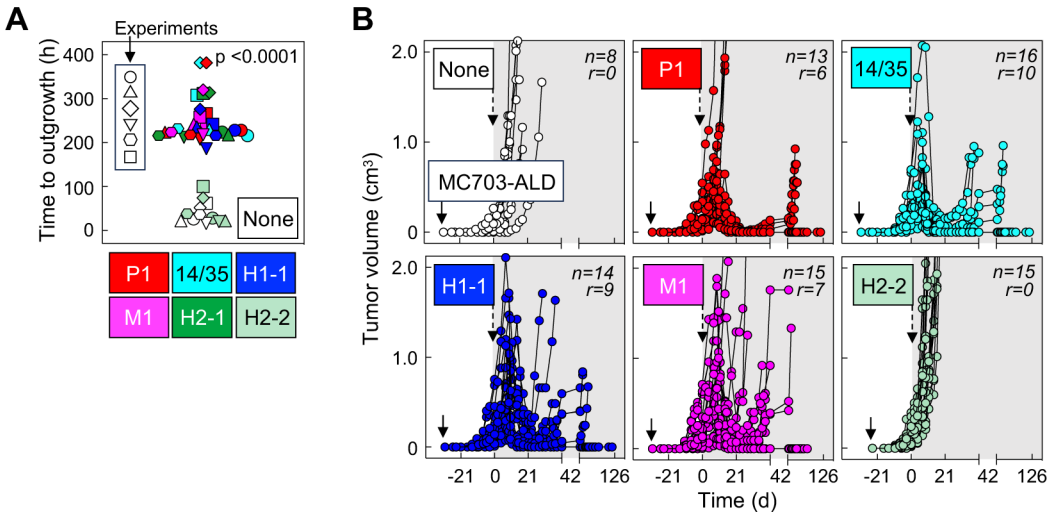


**Figure 5** Patient-derived TCRs that are specific for the neoantigen CDK4$^{R24L}$ display optimal in vivo efficacy. TCR-Ts were generated using TCRs derived from patients (P1 (red), 14/35 (cyan)), third party donors (H1-1 (blue), H2-1 (green), H2-2 (light green)) or humanized mice (M1, magenta). (A) Human TCR-Ts were incubated with WM-902B+A2 cancer cells and time to tumor outgrowth (≥15% confluence) was assessed by monitoring co-cultures using Incucyte SX5. Additional WM-902B+A2 cancer cells were added to the culture every 3 days. TCRs are color-coded and symbols refer to six independent experiments pooled in the depicted scatter plot. The p value results from unpaired t-test comparing TCRs predicted to be therapeutically effective (P1, 14/35, H1-1, H2-1, (M1) or failing (H2-2). (B) Mouse TCR-Ts were generated to assess TCR quality in vivo by adoptive therapy of TNA2 mice bearing large established MC703-ALD tumors. Shown are tumor growth curves pooled from two to three independent experiments. The number of treated mice in each group is shown in the upper right of each graph (n). The number of mice that rejected the tumor on transfer of TCR-Ts is stated below (r). Injection of MC703-ALD cancer cells is indicated with an arrow. The time of injecting TCR-Ts (color-coded for each TCR) is shown with a dashed arrow and was between 3 and 4 weeks after cancer cell inoculation. Mice receiving no T cells (None) are shown as control. The average tumor size at treatment start was 219±218 mm$^3$. TCR-Ts, T-cell receptor-modified T cells.

(referred to as M1) from a transgenic mouse that expressed the entire human TCR-α and TCR-β loci together with HLA-A2[26] and was immunized with the CDK4$^{R24L}$ NeoAg. We further used a validated patient-derived TCR from previous studies that developed in response to CDK4$^{R24C}$ but showed cross-reactivity to CDK4$^{R24L}$ (TCR 14/35[6 39]). The CDK4$^{R24L}$-specific TCRs were all unique with no apparent sequence similarities (table 2). We used this set of TCRs to verify whether long-term in vitro experiments would predict the therapeutic value of the different human CDK4$^{R24L}$-specific TCRs. TCR-Ts were generated by engineering human T cells obtained from peripheral blood of healthy donors (online supplemental figure 7A) and repeatedly challenged with cancer cells that endogenously expressed CDK4$^{R24L}$ (WM-902B+A2) (online supplemental figure 6). One TCR (H2-2) failed to inhibit cancer cell growth (figure 5A). All other TCRs (P1, 14/35, H1-1, H2-1, M1) similarly controlled tumor cell growth even after two consecutive re-challenges performed at 72 and 144 hours of the co-culture (figure 5A). TCRs from the effective group (derived from patients (P1, 14/35), or tumor-free environments (H1-1, M1)) were then tested in a syngeneic HLA-A2 (HHD)-transgenic mouse cancer model (TNA2[6]) and compared with TCR H2-2 that failed to inhibit cancer cell growth in vitro. TCR-Ts were generated by engineering T cells of HHD-transgenic mice (online supplemental figure 7B) and used to treat TNA2 mice bearing large established R24L-expressing tumors (MC703-ALD).[6] The group of TCRs predicted to be therapeutically effective was clearly distinguished from TCR H2-2. TCRs P1, 14/35, H1-1, and M1 induced tumor regression in most treated mice, followed by tumor rejection or relapse (figure 5B). The failing TCR H2-2 had no effect on tumor growth and in all treated mice MC703-ALD tumors progressed similarly to those growing in untreated mice (figure 5B).

## DISCUSSION

NeoAg-specific T-cell therapy using TCR-Ts holds promise as a highly effective treatment with minimal side effects,[40] but several challenges remain. Identifying optimal targets, such as immunodominant neoepitopes derived from driver mutations,[40] is difficult due to tumor heterogeneity[5] and the low expression levels of many proteins.[5 6] Furthermore, complete tumor rejection may require breaking immunodominance to identify TCRs that prevent tumor escape,[41] as well as employing combination strategies[8 41] and enhancing T-cell persistence. Nonetheless, selecting potent TCRs remains essential for robust therapeutic success.

Here we show that the NeoAg-specific T-cell repertoire in tumor-bearing hosts contains TCRs with divergent therapeutic efficacy when used for TCR therapy of established tumors. Infiltration and expansion of certain

T-cell clonotypes in the tumor did not correlate with therapeutic efficacy of their TCRs. Instead, persistent rather than immediate responses of TCR-Ts in vitro seemed to serve as a reliable parameter to identify TCRs that are therapeutically effective in vivo.

We made these observations with TCRs that were isolated in a mouse cancer model in which endogenous CD8 T cells interact with the H-2K$^b$-presented NeoAg mp68 in the tumor-bearing host for a period of up to 14.5 weeks. This model allows for the decoupling of tumor cell injection and presentation of mp68 to the immune system, so that exposure of the endogenous T-cell repertoire to mp68 in vivo occurs under non-inflammatory conditions. This is important because significant artifacts occur within the first days after tumor cell injection, including massive necrosis and acute inflammation.[34] These conditions favor the stimulation of the immune system and promote priming and expansion of tumor antigen-specific T cells; a situation that is unlikely to be found in patients with cancer. After about 2–3 weeks, when most transplanted tumors reach several millimeters in diameter, viable cancer and stromal cells typically replace these initial changes. By this time, the acute inflammatory response has subsided, and growing tumors are indistinguishable from autochthonous cancer. Exposing the immune system to a tumor antigen at this stage more closely mimics the situation in which tumor-specific T-cell repertoires evolve in patients. In the established model system, inducing mp68 expression 3 weeks after tumor cell injection had no effect on cancer progression. Infiltrating CD8 T cells expressed markers of exhaustion when analyzed 3–14.5 weeks later and contained a fraction that bound mp68-loaded tetramers. When analyzing the most expanded T-cell clonotypes within the mp68-specific TIL populations, their TCRs were surprisingly diverse, as no TCR was found twice, either within or in other tumor-bearing mice, thereby limiting the power to infer TCR quality based on specific sequence characteristics. However, such efforts may still be promising if more TCR sequences are generated from a T-cell repertoire, as this already allowed inferring specificity of certain TCR groups.[42] Here, we determined experimentally whether the tumor-derived TCRs were functionally comparable to TCRs from tumor-free environments generated by immunizing normal mice using the same cancer cells. Interestingly, more than half of the 13 tested TCRs (3 of 7 from TILs, 4 of 6 from immunized mice) were insufficient to destroy tumors when used in TCR therapy. The other proved to be therapeutically effective, regardless of whether they were derived from tumor-bearing or immunized mice, indicating that NeoAg-specific TCRs derived from tumors are not functionally inferior to TCRs generated in tumor-free environments. When testing for the function of TCR-Ts using in vitro assays, the therapeutic failure of a subset of TCRs (3 of 7) was not reliably predicted when measuring IFN-γ secretion after 24 hours incubation with target cells either loaded with graded amounts of mp68 peptide or tumor cells with ectopic or native mp68 expression. While both groups of therapeutically effective and failing TCRs could be statistically distinguished, relying on these short-term assays alone could run the risk of selecting clinical TCR candidates from a subgroup of outliers that are the result of inadequate test systems. This is in agreement with previous reports suggesting misinterpretation of T-cell function by labeling with MHC tetramers.[43–45] We therefore extended our analysis to include T-cell stress tests, comparable to those used for characterizing T cells expressing chimeric antigen receptors.[46] Here, we exposed TCR-Ts to fresh tumor cells in repeating cycles to determine which TCR-Ts were most effective in suppressing cancer cell growth in vitro over time. In contrast to the short-term assays, these experiments lasted up to 15 days, covering the period during which TCR-Ts are typically seen to initiate tumor destruction in vivo. These experiments proved to be an accurate predictor of therapeutic efficacy in vivo, as they allowed effective and failing TCRs to be clearly differentiated. None of the failing TCRs inhibited growth of cancer cells on initial co-culture, while all effective TCRs suppressed cancer growth even after one or even two re-challenges.

For the analysis of human TCRs, in vivo test systems to evaluate the therapeutic efficacy of TCR-Ts are difficult to obtain. We previously established an HLA-A2-transgenic mouse cancer model to analyze human TCRs and antigens under syngeneic conditions for use in TCR therapy.[6] In this model, all molecules involved in antigen recognition are human, while all cellular components are mouse. In previous studies, this model has already proven useful for assessing the quality of different tumor antigens and TCRs,[27 47 48] such as the characterization of the HLA-A2-presented NeoAg CDK4$^{R24L}$ as a suitable target for TCR therapies.[6] Here, we used this model to benchmark the predictive power of long-term stress tests by determining the in vivo function of NeoAg-specific TCR-Ts. A critical factor for the establishment of NeoAg-specific TCR therapies is that autologous TCRs are in some cases difficult to obtain, as sufficient patient material is not always available to isolate T cells, or the frequency of NeoAg-specific T cells is too low to be isolated. TCRs isolated from HLA-matched T cells of third-party donors[18 38 49 50] or MHC-transgenic, humanized mice[26 27] are possible alternatives. However, this would require a comprehensive safety profile of these non-autologous receptors to exclude cross-reactivity with combinations of allogeneic MHC and self-antigens that may be presented by normal tissues of the patient.[48] Here we studied a panel of CDK4$^{R24L}$-specific TCRs derived from either TILs or tumor-free environments. When performing long-term assays to evaluate TCR-T persistence, only one TCR derived from T cells of a third-party donor was unable to prevent tumor cell outgrowth, while all others overcame two or even three re-challenges with cancer cells. Analysis of TCR-Ts in vivo using the TNA2 mouse cancer model confirmed the predicted TCR quality. While this underlines the predictive power of long-term analyses, the panel of five

in vivo-tested CDK4$^{R24L}$-specific TCRs was insufficient to demonstrate superiority over short-term experiments, as the only TCR that failed in animal studies also exhibited a low $EC_{50}$ value in previous analyses.[18] Importantly, the quality of two TCRs derived from patients was equivalent to that of TCRs isolated from a tumor-free environment. Thus, the use of autologous NeoAg-specific TCRs for TCR therapy is compatible with optimal therapeutic efficacy.

**Author affiliations**
[1]Institute of Immunology, Charité - Universitätsmedizin Berlin, Berlin, Germany
[2]Department of Internal Medicine III, University Hospital Regensburg, Regensburg, Germany
[3]German Cancer Consortium (DKTK), Partner site Berlin, and German Cancer Research Center (DKFZ), Heidelberg, Germany
[4]Department of Pathology, The University of Chicago, Chicago, Illinois, USA
[5]David and Etta Jonas Center for Cellular Therapy, The University of Chicago, Chicago, Illinois, USA
[6]The Pritzker School of Molecular Engineering, The University of Chicago, Chicago, Illinois, USA
[7]Cancer Precision Medicine, Inc, Tokyo, Japan
[8]Department of Cancer Immunology, Institute for Cancer Research, Oslo University Hospital Radiumhospitalet, Oslo, Norway
[9]Department of Medicine, Center for Personalized Therapeutics, The University of Chicago, Chicago, Illinois, USA
[10]Department of Neurology, Bursky Center for Human Immunology, and Immunotherapy Programs, Hope Center for Neurological Disorders, Center for Brain Immunology and Glia, Siteman Cancer Center, Washington University School of Medicine, St. Louis, Missouri, USA
[11]Department of Urology, Osaka University Graduate School of Medicine, Osaka, Japan
[12]Precision Immunotherapy Alliance, University of Oslo, Oslo, Norway
[13]Cancer Precision Medicine Center, Japanese Foundation for Cancer Research, Tokyo, Japan
[14]Molecular Immunology and Gene Therapy, Max-Delbrück-Center for Molecular Medicine in the Helmholtz Association, Berlin, Germany
[15]Committee on Cancer Biology and Committee on Immunology, The University of Chicago, Chicago, Illinois, USA

**Present affiliations** The present affiliation of Xinyi Feng is: Center for Immunology and Inflammatory Diseases, Massachusetts General Hospital and Program in Immunology, Harvard Medical School, Boston, MA, USA; Taigo Kato is: Department of Urology, Osaka University Graduate School of Medicine, Osaka, Japan and Yusuke Nakamura is: Center for Intractable Diseases and Immunogenomics, National Institute of Biomedical Innovation, Health and Nutrition, Ibaraki-shi, Osaka, Japan.

**Acknowledgements** We thank Wolfgang Uckert for his initial support of the project and Kordelia Hummel for her technical assistance. We thank Ton Schumacher and Pia Kvistborg for providing TCR P17 for this study. We thank Thomas Schüler for valuable feedback and discussion. We thank the Core Facility for flow cytometry at the Max-Delbrück-Center for Molecular Medicine, and especially Hans Peter Rahn, for support in cell sorting. We also thank Kerstin Dietze for her technical support in establishing TCR sequencing from single T cells. The authors thank the staff of the Animal Facility at the MDC, specifically Isabell Höft, for their assistance in performing animal experiments.

**Contributors** Conception and design: LR, TB, HS, ML. Experiments and methodology: LR, SPW, KD, CM, XF, GC, PYY, ES, TK, NS, GW. Analysis and interpretation of data: LR, LH, SPW, VA, JH, JO, YN, GW, ML. Writing of the original draft: LR, ML. Review and editing: all authors. ML is the guarantor.

**Funding** This work was supported by the NIH (R01-CA22677) (ML, HS), the Deutsche Forschungsgemeinschaft (project number: 409512914) (ML), the David and Etta Jonas Center for Cellular Therapy at The University of Chicago (ML, HS), the German Cancer Consortium (ML), the Einstein Foundation Berlin (A-2019-559) (ML), and Deutsche Krebshilfe e.V. (70113355) (LH). We further acknowledge start-up grants from The University of Chicago and the Chicago Immunoengineering Innovation Center (both JH). Additional grant support was provided by the European Research Council under the European Union's Horizon 2020 research and innovation program (grant agreement No. 882963 to TB and No. 865805 to JO), and by the Cancer Grand Challenges partnership funded by CRUK (CGCATF-2023/100011) and the National Cancer Institute (1OT2CA297513-01), as members of the MATCHMAKERS team (JO).

**Competing interests** ML is a recipient of grant/research support from T-knife GmbH. LH serves on advisory boards for Bristol Myers Squibb, Gilead, Johnson & Johnson, Pierre-Fabre and Sanofi and has received travel support from Amgen, Gilead and Johnson & Johnson. TB is a founder and scientific advisory board member of T-knife Therapeutics.

**Patient consent for publication** Not applicable.

**Ethics approval** Not applicable.

**Provenance and peer review** Not commissioned; externally peer reviewed.

**Data availability statement** Data are available upon reasonable request.



**ORCID iDs**
Steven P Wolf http://orcid.org/0009-0008-2723-695X
Jun Huang http://orcid.org/0000-0003-0271-4384
Erlend Strønen http://orcid.org/0000-0001-9314-9389
Gerald Willimsky http://orcid.org/0000-0002-9693-948X
Matthias Leisegang http://orcid.org/0000-0003-3692-7142

## REFERENCES

1 Alexandrov LB, Nik-Zainal S, Wedge DC, *et al*. Signatures of mutational processes in human cancer. *Nature New Biol* 2013;500:415–21.
2 Monach PA, Meredith SC, Siegel CT, *et al*. A unique tumor antigen produced by a single amino acid substitution. *Immunity* 1995;2:45–59.
3 Dubey P, Hendrickson RC, Meredith SC, *et al*. The immunodominant antigen of an ultraviolet-induced regressor tumor is generated by a somatic point mutation in the DEAD box helicase p68. *J Exp Med* 1997;185:695–705.
4 Parkhurst MR, Robbins PF, Tran E, *et al*. Unique Neoantigens Arise from Somatic Mutations in Patients with Gastrointestinal Cancers. *Cancer Discov* 2019;9:1022–35.
5 Leisegang M, Engels B, Schreiber K, *et al*. Eradication of Large Solid Tumors by Gene Therapy with a T-Cell Receptor Targeting a Single Cancer-Specific Point Mutation. *Clin Cancer Res* 2016;22:2734–43.
6 Leisegang M, Kammertoens T, Uckert W, *et al*. Targeting human melanoma neoantigens by T cell receptor gene therapy. *J Clin Invest* 2016;126:83465:854–8:.
7 Schreiber K, Karrison TG, Wolf SP, *et al*. Impact of TCR Diversity on the Development of Transplanted or Chemically Induced Tumors. *Cancer Immunol Res* 2020;8:192–202.
8 Wolf SP, Anastasopoulou V, Drousch K, *et al*. One CD4+TCR and One CD8+TCR Targeting Autochthonous Neoantigens Are Essential and Sufficient for Tumor Eradication. *Clin Cancer Res* 2024;30:1642–54.
9 Martinov T, Greenberg PD. Targeting Driver Oncogenes and Other Public Neoantigens Using T Cell Receptor-Based Cellular Therapy. *Annu Rev Cancer Biol* 2023;7:331–51.
10 Foy SP, Jacoby K, Bota DA, *et al*. Non-viral precision T cell receptor replacement for personalized cell therapy. *Nature New Biol* 2023;615:687–96.
11 Parkhurst M, Goff SL, Lowery FJ, *et al*. Adoptive transfer of personalized neoantigen-reactive TCR-transduced T cells in metastatic colorectal cancer: phase 2 trial interim results. *Nat Med* 2024;30:2586–95.

12 Espinosa-Carrasco G, Chiu E, Scrivo A, *et al*. Intratumoral immune triads are required for immunotherapy-mediated elimination of solid tumors. *Cancer Cell* 2024;42:1202–16.
13 Wolf SP, Leisegang M, Steiner M, *et al*. CD4+ T cells with convergent TCR recombination reprogram stroma and halt tumor progression in adoptive therapy. *Sci Immunol* 2024;9:eadp6529.
14 Willimsky G, Blankenstein T. Sporadic immunogenic tumours avoid destruction by inducing T-cell tolerance. *Nature New Biol* 2005;437:141–6.
15 Willimsky G, Czéh M, Loddenkemper C, *et al*. Immunogenicity of premalignant lesions is the primary cause of general cytotoxic T lymphocyte unresponsiveness. *J Exp Med* 2008;205:1687–700.
16 Rudloff MW, Zumbo P, Favret NR, *et al*. Hallmarks of CD8+ T cell dysfunction are established within hours of tumor antigen encounter before cell division. *Nat Immunol* 2023;24:1527–39.
17 Engels B, Cam H, Schüler T, *et al*. Retroviral vectors for high-level transgene expression in T lymphocytes. *Hum Gene Ther* 2003;14:1155–68.
18 Strønen E, Toebes M, Kelderman S, *et al*. Targeting of cancer neoantigens with donor-derived T cell receptor repertoires. *Science* 2016;352:1337–41.
19 Cohen CJ, Zhao Y, Zheng Z, *et al*. Enhanced antitumor activity of murine-human hybrid T-cell receptor (TCR) in human lymphocytes is associated with improved pairing and TCR/CD3 stability. *Cancer Res* 2006;66:8878–86.
20 Heinz N, Schambach A, Galla M, *et al*. Retroviral and transposon-based tet-regulated all-in-one vectors with reduced background expression and improved dynamic range. *Hum Gene Ther* 2011;22:166–76.
21 Pascolo S, Bervas N, Ure JM, *et al*. HLA-A2.1-restricted education and cytolytic activity of CD8(+) T lymphocytes from beta2 microglobulin (beta2m) HLA-A2.1 monochain transgenic H-2Db beta2m double knockout mice. *J Exp Med* 1997;185:2043–51.
22 Morita S, Kojima T, Kitamura T. Plat-E: an efficient and stable system for transient packaging of retroviruses. *Gene Ther* 2000;7:1063–6.
23 Hennig K, Raasch L, Kolbe C, *et al*. HEK293-based production platform for γ-retroviral (self-inactivating) vectors: application for safe and efficient transfer of COL7A1 cDNA. *Hum Gene Ther Clin Dev* 2014;25:218–28.
24 Letourneur F, Malissen B. Derivation of a T cell hybridoma variant deprived of functional T cell receptor alpha and beta chain transcripts reveals a nonfunctional alpha-mRNA of BW5147 origin. *Eur J Immunol* 1989;19:2269–74.
25 Percie du Sert N, Hurst V, Ahluwalia A, *et al*. The ARRIVE guidelines 2.0: Updated guidelines for reporting animal research. *PLoS Biol* 2020;18:e3000410.
26 Li L-P, Lampert JC, Chen X, *et al*. Transgenic mice with a diverse human T cell antigen receptor repertoire. *Nat Med* 2010;16:1029–34.
27 Obenaus M, Leitão C, Leisegang M, *et al*. Identification of human T-cell receptors with optimal affinity to cancer antigens using antigen-negative humanized mice. *Nat Biotechnol* 2015;33:402–7.
28 Penter L, Dietze K, Ritter J, *et al*. Localization-associated immune phenotypes of clonally expanded tumor-infiltrating T cells and distribution of their target antigens in rectal cancer. *Oncoimmunology* 2019;8:e1586409.
29 Han A, Glanville J, Hansmann L, *et al*. Linking T-cell receptor sequence to functional phenotype at the single-cell level. *Nat Biotechnol* 2014;32:684–92.
30 Saligrama N, Zhao F, Sikora MJ, *et al*. Opposing T cell responses in experimental autoimmune encephalomyelitis. *Nature New Biol* 2019;572:481–7.
31 Lefranc MP. IMGT, the International ImMunoGeneTics Information System. *Cold Spring Harb Protoc* 2011;2011:595–603.
32 Schreiber K, Arina A, Engels B, *et al*. Spleen cells from young but not old immunized mice eradicate large established cancers. *Clin Cancer Res* 2012;18:2526–33.
33 Schreiber K, Wu TH, Kast WM, *et al*. Tracking the common ancestry of antigenically distinct cancer variants. *Clin Cancer Res* 2001;7:871s–75s.
34 Schreiber K, Rowley DA, Riethmüller G, *et al*. Cancer immunotherapy and preclinical studies: why we are not wasting our time with animal experiments. *Hematol Oncol Clin North Am* 2006;20:567–84.
35 Philip M, Schietinger A. CD8+ T cell differentiation and dysfunction in cancer. *Nat Rev Immunol* 2022;22:209–23.
36 Pasetto A, Gros A, Robbins PF, *et al*. Tumor- and Neoantigen-Reactive T-cell Receptors Can Be Identified Based on Their Frequency in Fresh Tumor. *Cancer Immunol Res* 2016;4:734–43.
37 Kvistborg P, Shu CJ, Heemskerk B, *et al*. TIL therapy broadens the tumor-reactive CD8(+) T cell compartment in melanoma patients. *Oncoimmunology* 2012;1:409–18.
38 Ali M, Foldvari Z, Giannakopoulou E, *et al*. Induction of neoantigen-reactive T cells from healthy donors. *Nat Protoc* 2019;14:1926–43.
39 Wölfel T, Hauer M, Schneider J, *et al*. A p16INK4a-insensitive CDK4 mutant targeted by cytolytic T lymphocytes in a human melanoma. *Science* 1995;269:1281–4.
40 Blankenstein T, Leisegang M, Uckert W, *et al*. Targeting cancer-specific mutations by T cell receptor gene therapy. *Curr Opin Immunol* 2015;33:112–9.
41 Friedman J, Moore EC, Zolkind P, *et al*. Neoadjuvant PD-1 Immune Checkpoint Blockade Reverses Functional Immunodominance among Tumor Antigen-Specific T Cells. *Clin Cancer Res* 2020;26:679–89.
42 Glanville J, Huang H, Nau A, *et al*. Identifying specificity groups in the T cell receptor repertoire. *Nature New Biol* 2017;547:94–8.
43 Derby MA, Wang J, Margulies DH, *et al*. Two intermediate-avidity cytotoxic T lymphocyte clones with a disparity between functional avidity and MHC tetramer staining. *Int Immunol* 2001;13:817–24.
44 Wilde S, Sommermeyer D, Leisegang M, *et al*. Human antitumor CD8+ T cells producing Th1 polycytokines show superior antigen sensitivity and tumor recognition. *J Immunol* 2012;189:598–605.
45 Hombrink P, Raz Y, Kester MGD, *et al*. Mixed functional characteristics correlating with TCR-ligand koff -rate of MHC-tetramer reactive T cells within the naive T-cell repertoire. *Eur J Immunol* 2013;43:3038–50.
46 Kiesgen S, Messinger JC, Chintala NK, *et al*. Comparative analysis of assays to measure CAR T-cell-mediated cytotoxicity. *Nat Protoc* 2021;16:1331–42.
47 Gavvovidis I, Leisegang M, Willimsky G, *et al*. Targeting Merkel Cell Carcinoma by Engineered T Cells Specific to T-Antigens of Merkel Cell Polyomavirus. *Clin Cancer Res* 2018;24:3644–55.
48 Foldvari Z, Knetter C, Yang W, *et al*. A systematic safety pipeline for selection of T-cell receptors to enter clinical use. *NPJ Vaccines* 2023;8:126.
49 Anczurowski M, Hirano N. Two Weeks' Notice from Allogeneic Sources. *Clin Cancer Res* 2018;24:5195–7.
50 Matsuda T, Leisegang M, Park J-H, *et al*. Induction of Neoantigen-Specific Cytotoxic T Cells and Construction of T-cell Receptor-Engineered T Cells for Ovarian Cancer. *Clin Cancer Res* 2018;24:5357–67.